CGMS-XXXII
PRC-WP-07
Prepared by CMA

# Destripe Multi-Sensor Imaging Spectroradiometer Data


Summary and purpose of paper

This paper gives the method to destripe the data of multi-sensor imaging spectroradiometer on SZ-3, similar instruments will also fly on future FY-3 satellites. The method used is similar to the method developed by Weinreb (et al. 1989) of NESDIS for GOES satellite.

# Destripe Multi-Sensor Imaging Spectroradiometer Data

Zhu Xiaoxiang, Fan Tianxi, Huang Qian
National Satellite Meteorological Center
Beijing 100081, China
zhuxx@nsmc.cma.gov.cn

## 1. Introduction

Striping is a common problem faced by imaging spectroradiometer on spacecrafts, and it affects the data usage. Periodic striping on the imagery becomes prominent with time on. Differential sensitivity of sensors to the incoming radiation is the reason behind and therefore this phenomenon is unavoidable with multi-sensor instruments. Striping on imagery affects calibration, too. To destripe imagery data is an important task before any quantitative usage of the data.

## 2. Method

Several methods have been available, like the one by Horn et al 1979 that uses histogram modification to destripe Landsat MSS images. Kautsky et al (1984) developed a method by smoothed histogram modification for image processing. In 1989, Weinreb et al destriped GOES image by matching empirical distribution functions. In the same year, Crippen[4] used simple spatial filtering routine for the cosmetic removal of scan-line noise from Landsat TM P-tape imagery. Wegener (1990) [5] used improved histogram matching to destripe multiple sensor imagery. In 1998, Srinivassan et al.[6] destriped Landsat data by using power filtering. Gadallah et al.[7] (2000) developed a way with moment matching, Liu et al. [8] (2002) improved this way.

In our approach, we destripe imaging spectroradiometer data of SZ-3 by matching empirical distribution function, which is developed by Weinreb et al. in 1989.

Theoretically, when several sensors view the same scene, their outputs should be equal, and this should be no matter what the scene is. This is an ideal condition. Practically there is always difference in the outputs, being caused mainly by the physical and mechanical performances of sensors, synthetically called sensitivity. No two sensors ever view exactly the same scene actually. However, for a large ensemble of measurements, the distribution of the intensity of the earth radiation incident on each sensor will be similar. With this assumption, the distributions of the outputs of each sensor should be identical.

Therefore, when one sensor’s distribution of the intensity is known, the others are presumably the same. The key point is to select a standard sensor among all sensors. Considering the performance of sensors, the standard one should be chosen in terms of its relative stabilization, low noise, and maximal use of the dynamic range of the data system without clipping either at the low or high ends. According to the distribution, the outputs of other sensors can be adjusted with normalization tables.

To calculate the sensor’s distribution of the intensity, an Empirical Distribution

Function (EDF) is defined as a cumulative intensity for every count. It can be expressed as

$$P_i(x) = \sum_{y=0}^{x} p_i(y) \qquad \textbf{( 1)}$$

where the subscript *i* refers to sensor number, $p_i(y)$ is the intensity for count *x* of sensor *i*, $P_i(x)$ is the cumulative intensity of those counts from 0 to *x*. This function is a non-decreasing function of x, and its maximum value is unity. Here, we choose the maximum value to be 1. It means when output *x* equals to X, then

$$P_i(X) = 1 \qquad \textbf{( 2)}$$

According to the assumption, each output value *x* in sensor *i*, the normalizes value *x'* should satisfy

$$P_s(x') = P_i(x) \qquad \textbf{( 3)}$$

where the subscripts refers to the standard sensor. In practice, not only is $P_s$ non-decreasing, but is also monotonically increasing as a function of *x'* in the domain of *x'* where there are data. Consequently, it can be inverted, and the solution for *x'* can be written as

$$x' = P_s^{-1}[(P_i(x)] \qquad \textbf{(4)}$$

Equation(4) shows the relation between *x* and *x'*, this is the basis to generate a

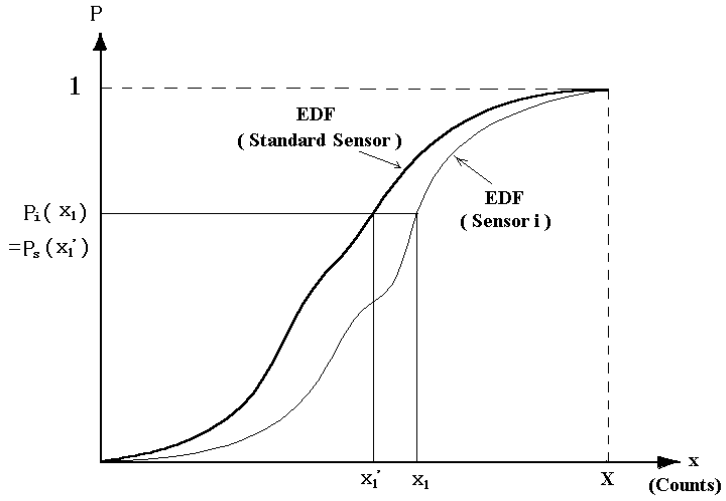


Fig 1. Illustration of procedure to generate normalization look-up table

normalization look-up table relating each *x* and *x'*. Figure 1 illustrates how it works in

actual practice to generate the content in the table. The figure show us the idealized EDFs for standard sensor and sensor *i*. The EDF curves in the figure are continuous, however, they are discrete in practice because the counts (*x*) are integers. For this reason, it should be interpolated within the EDF of standard sensor to find the value of *x'* that *x* corresponds.

Another roughly factor of 2 growth in pixel size as Instantaneous Field Of-View (IFOV) varies from nadir to two edges leads to a 'bowtie' effect, the scans are shown schematically in Figure 2. The result is that nearly 40%of the Imaging Spectroradiometer pixels overlap.

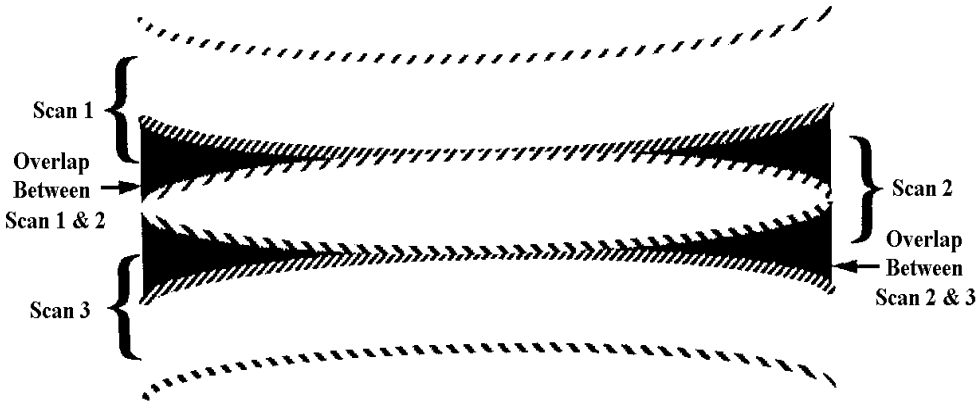


Figure 2. Schematic of Overlap in SZ-3 Imaging Spectroradiometer Scans

In order to eliminate this phenomenon, an empirical method is developed after we analyzed the characters of data. It is known that the overlapped area becomes larger when it is closer to both edges, mainly, it is caused by both curvature of earth effect and observation distance change. We assume that every scan in nadir are matched precisely and pixel size has a bilinear relation with scanning (pixels) and moving (sensors) direction. For a stable platform and instrument, the overlapped widths (number lines) in both edges should be equal and fixed. So the displacement of every pixel can be calculated by the under formula:

$$\Delta I = (N_s - N_{cs}) / C_1 \times (|\, N_p - N_{cp}\,|) / C_2 \times \Delta P \qquad (5)$$

Where $N_s$ is the number of every sensor, for example, the value of SZ-3 Imaging Spectroradiometer is from 1 to 22. $N_{cs}$ is the central number sensor, normally, the value is half of total sensors. $N_p$ is the number of pixel in scanning direction, $N_{cp}$ is the central pixel number in every scan line, normally the value is half total pixels of the line. $C_1$ and $C_2$ are constants, their values are same as $N_{cs}$ and $N_{cp}$. $\Delta P$ is

the number of overlapped pixels, its value is half of the overlapped widths.

## 3. Data Process and Analysis

Imaging spectroradiometer on SZ-3 has 34 channels, 30 channels locate in visible and near-infrared band, arranging from 401nm to 1018nm. Both interval and the width between the channels are about 20nm. The other 4 channels are infrared, 2.15~2.25μm, 8.4~8.9μm, 10.3~11.3μm and 11.5~12.5μm. The spatial resolution at

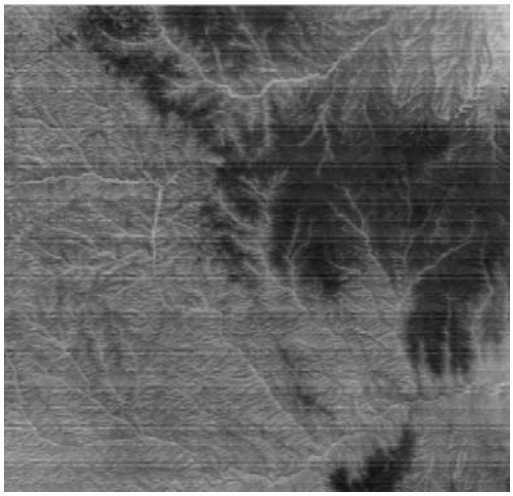

Fig 3. Raw image of channel 3 for imaging spectrometer data of SZ-3

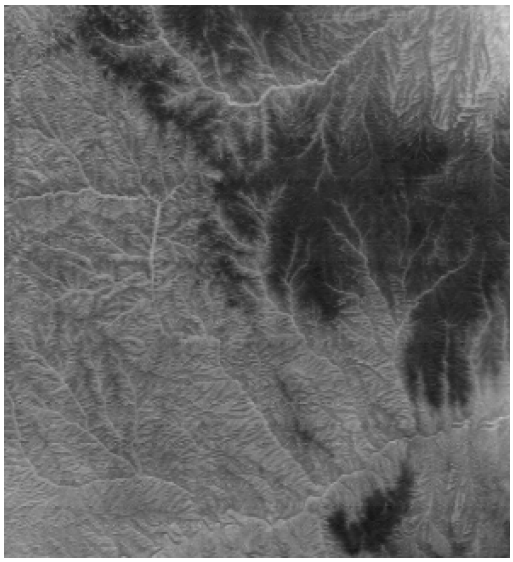

Fig 5. Normalized image, others are same as Fig. 3.

nadir is 500m, every channel scanner has 22 sensors. The data dynamic range is from 0 to 4095 (12 bit). Figure 3 shows part of an image of channel 3 (440-460nm), periodic striping is obvious, the width is 22 lines, the same number as of the sensors.

After analyzing every sensor data, we find sensor 3 is the best one, so this sensor is selected as standard sensor.

By using above method, we get EDFs for every sensor and look-up table, Figure 4 shows the EDFs for three sensors, others have the similar shapes.

After adjusted by look-up table, image looks much better than unnormalized image. Figure 5 is the normalized image.

Figure 6(a), (b) and (c) show the difference among composite image of raw data, destriped data and resampled data. It is easy to find that stripes and 'bowtie' lakes on Figure 6(a). After destriping, stripes disappear and 'bowtie' lakes are still on it as Figure 6(b) shows. Finally, resampling is done and 'bowtie' lakes also disappear.

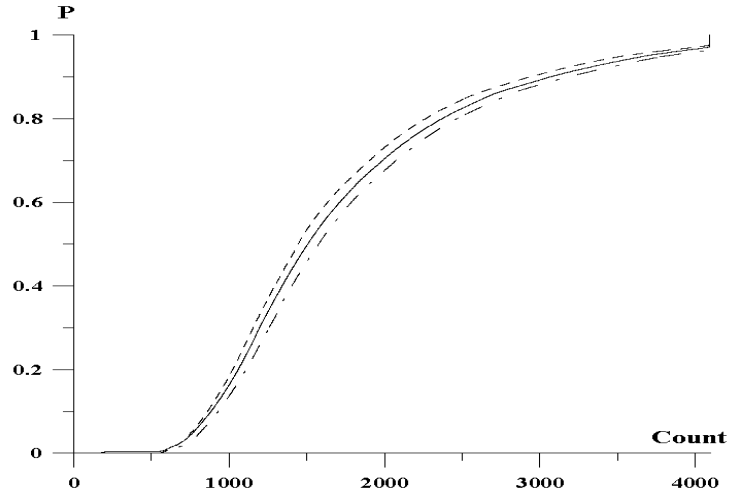


Fig 4. Empirical distribution functions at channel 15 for unnormalized parts of sensors data for SZ-3 76$^{th}$ orbit, (- - -) Sensor 1, (—) Sensor 3, (- · - ·) Sensor 22

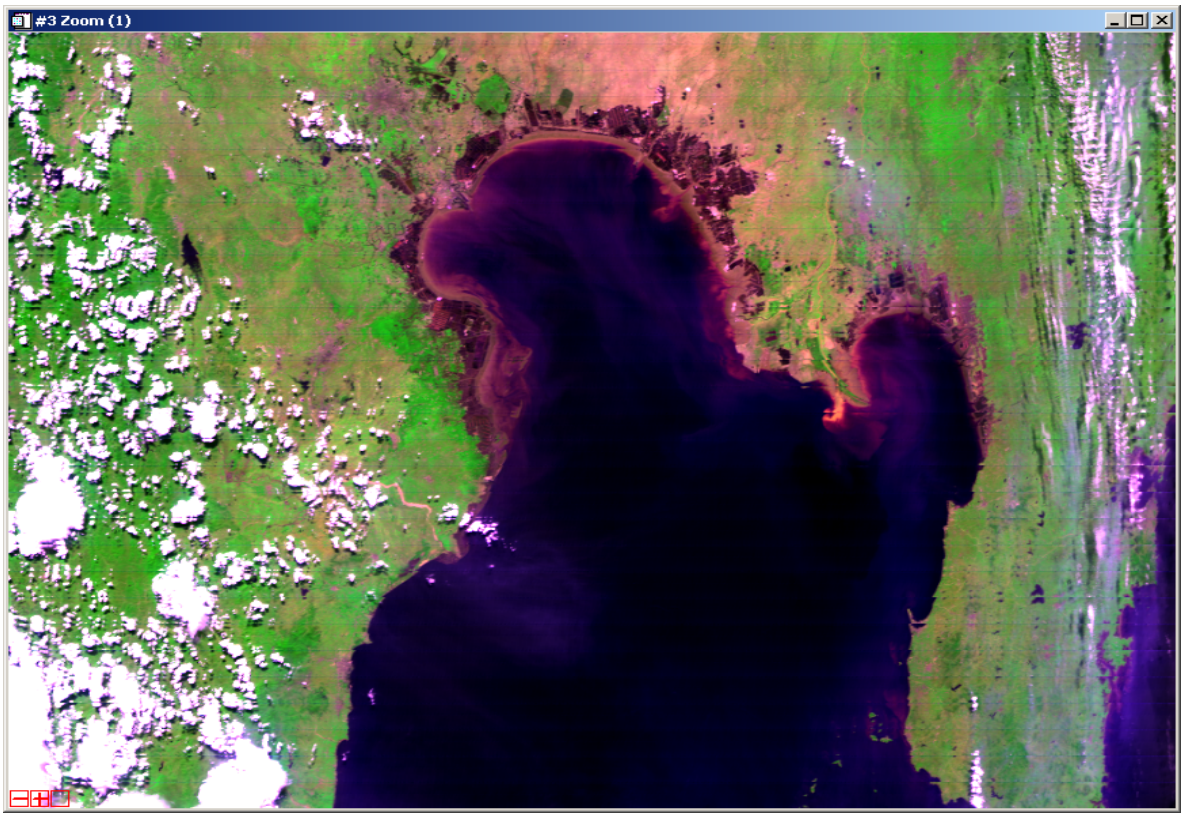


(a) Raw data composite image

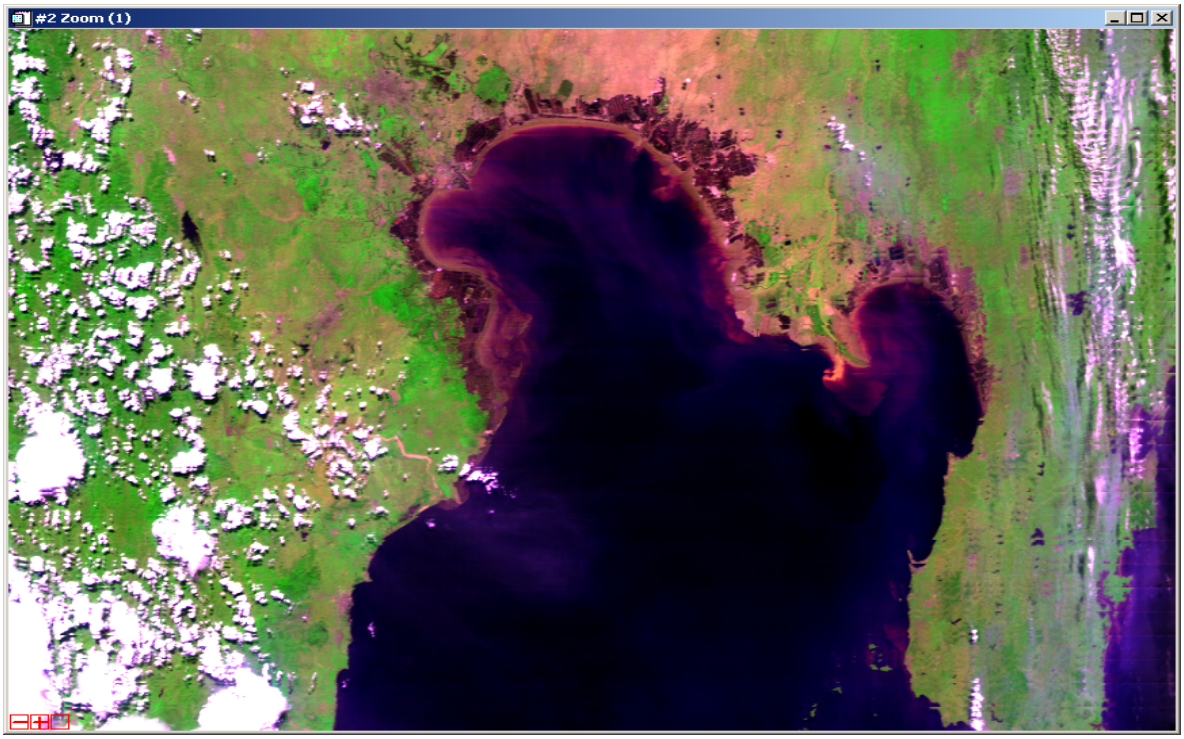


(b) Destriped data composite image

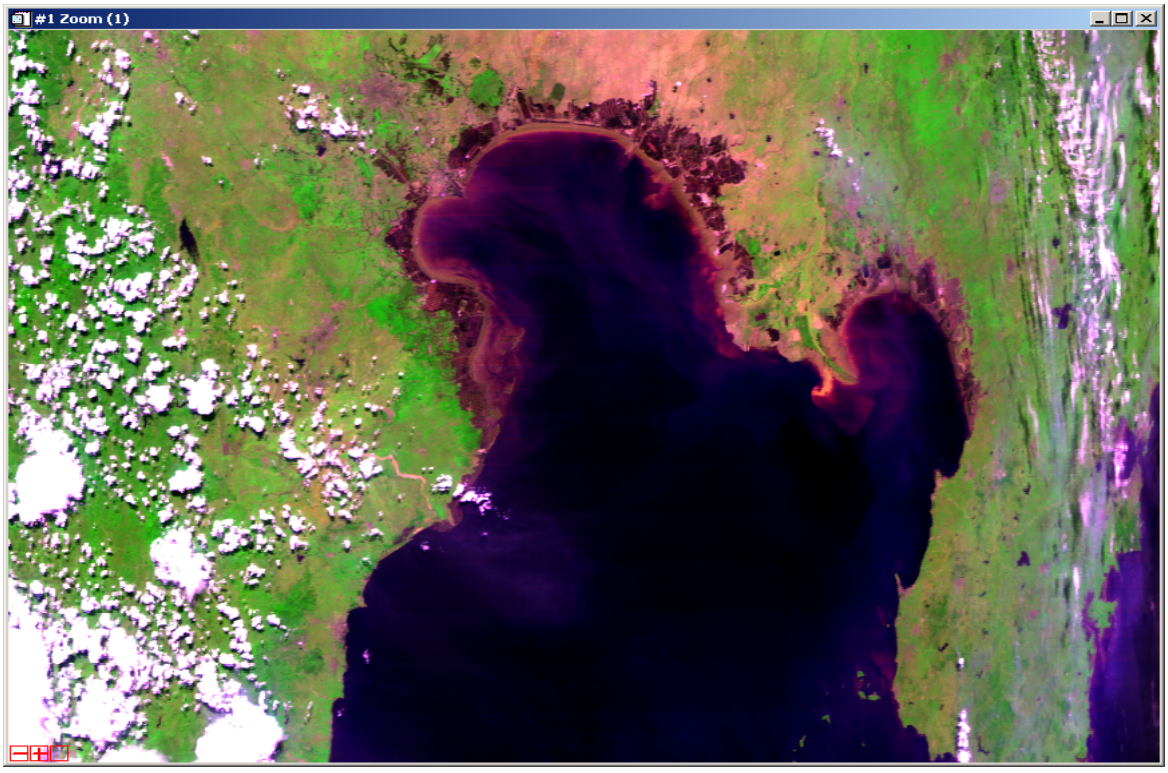


(c) Composite image after destriping and resampling

Figure 6. Comparison among raw, destriped and resampled composite image of SZ-3 Imaging Spectrometer
Channel 15, 20, 3 (RGB)

## 4.Conclusion

Nearly one hundred SZ-3 Imaging Spectrometer orbit data have been processed using above method, and the results show that the method is applicable. The quality of raw data and their images are improved. This method will give some help in calibrating different sensors. It also help us prepare scheme for processing the similar instrument data from FY-3, the next generation polar orbit meteorological satellite of China.

## REFERENCES

[1] B.K.P.Horn, R.J.Woodham. Destriping Landsat MSS images by histogram modification [J]. Comput. Graph.& Image Process., 1979, vol.10: 69-83

[2] J.Kautsky, N.K.Nichols, D.L.B.Jupp. Smoothed histogram modification for image processing [J]. Comput. Vis. & Image Process., 1984, vol.26: 271-291

[3] Weinreb M P, Xie R, Lienesch, J H et al. Destriping GEOS Images by Matching Empirical Distribution Functions. Remote Sens. Environ. 1989, 29:185-195.

[4] Robert E. Crippen. Simple Spatial Filtering Routine for the Cosmetic Removal of Scan-Line Noise from Landsat TM P-Tape Imagery [J]. Photogrammetric Engineering & Remote Sensing, 1989, vol.55(3): 327-331

[5] Michael Wegener, Destriping multiple sensor imagery by improved histogram matching. Int. J. Remote sensing, 1990, Vol. 11, No. 5859-5875;

[6] Srinivasan, R., Cannon, M., White, J., Landsat data destriping using power filtering [J]. Optical Engineering, 1998, vol.27: 939-943

[7] F.L.Gadallah, F.Csillag, E.J.M.Smith. Destriping multisensor imagery with moment matching [J]. Int. J. Remote Sensing, 2000, vol.21(12): 2505-2511.

[8] Liu Zhengjun, Wang Changyao, Wang Chen. Destriping Imaging Spectrometer Data By An Improved Moment Matching Method. Journal of Remote Sensing 2002，6（4）：279~284.

[9] Draft of the MODIS Level 1B Algorithm Theoretical Basis Document Version 2.0[ATBMOD-01], Feb. 13 1997, SAIC/GSC MCST Document.